1) With $U_j = e^{\frac{i}{2}\frac{\pi}{2}\sigma_j^y} = \frac{1}{\sqrt{2}}(\mathbb{1}_j + i\sigma_j^y)$ and

$$e^{i\hat{n}\cdot\vec{\sigma}\frac{\varphi}{2}} = \cos\left(\frac{\varphi}{2}\right)\mathbb{1} + i\sin\left(\frac{\varphi}{2}\right)\hat{n}\cdot\vec{\sigma}$$

$[\sigma^\mu, \sigma^\nu] = 2i\,\varepsilon_{\mu\nu\rho}\,\sigma^\rho$, we directly get

$$U_j\,\sigma_j^x\,U_j^\dagger = \frac{1}{2}(\mathbb{1} + i\sigma^y)\,\sigma^x(\mathbb{1} - i\sigma^y) =$$

[drop $j$]

$$= \frac{1}{2}\left(\sigma^x + \sigma^y\sigma^x\sigma^y + i[\sigma^y, \sigma^x]\right) = \sigma^z,$$

($\sigma^y\sigma^x\sigma^y = -\sigma^x$, $i[\sigma^y, \sigma^x] = 2\sigma^z$)

and similarly $U_j\,\sigma_j^z\,U_j^\dagger = -\sigma_j^x$.

The transformed Hamiltonian $H' = U H U^\dagger$ with $U = \bigotimes_j U_j$ then reads as

$$H' = -J \sum_j \sigma_j^x \sigma_{j+1}^x - h \sum_j \sigma_j^z .$$

$\sigma_j^x = \sigma_j^+ + \sigma_j^-$

On using the Jordan Wigner substitutions, we get

$$H'_{JW} = -J \sum_{j=1}^{L-1} (c_j^\dagger + c_j)(c_{j+1}^\dagger + c_{j+1}) - h \sum_{j=1}^{L} (2 c_j^\dagger c_j - 1)$$

$$= hL - 2h \sum_{j=1}^{L} c_j^\dagger c_j - J \sum_{j=1}^{L-1} [(c_j^\dagger - c_j)(c_{j+1}^\dagger + c_{j+1})]$$

$$= c_j^\dagger c_{j+1} + c_j^\dagger c_{j+1}^\dagger + \text{h.c.}$$

$c_j^\dagger F_j = -F_j c_j^\dagger = c_j^\dagger$

$c_j F_j = -F_j c_j = -c_j$

$\{c_i, c_\ell^\dagger\} = 2\delta_{i\ell}$

Periodic boundaries:

$$-J\left(\sigma_L^+ + \sigma_L^-\right)\left(\sigma_1^+ + \sigma_1^-\right) =$$

$$= -J(-1)^{\sum_{j<L} c_j^+ c_j}\left(c_L^+ + c_L\right)\left(c_1^+ + c_1\right) =$$

$$= J(-1)^{\sum_{j=1} n_j}\left(c_L^+ - c_L\right)\left(c_1^+ + c_1\right) =$$

$$= J(-1)^{\sum_{j=1} n_j}\left(c_L^+ c_1 + c_L^+ c_1^+ + h.c.\right)$$

2) Introduce Nambu-spinors $\eta_j = \begin{pmatrix} c_j \\ c_j^+ \end{pmatrix}$, then

$$c_j^+ c_j = \frac{1}{2}\left(c_j^+ c_j - c_j c_j^+ + 1\right) = \frac{1}{2}\eta_j^+ \tau_z \eta_j + \frac{1}{2}$$

($\tau_z$: Pauli-matrix)

$$c_j^+ c_{j+1} = \text{---} = \frac{1}{2}\left(\eta_j^+ \tau_z \eta_{j+1} + h.c.\right)$$

Interlude:

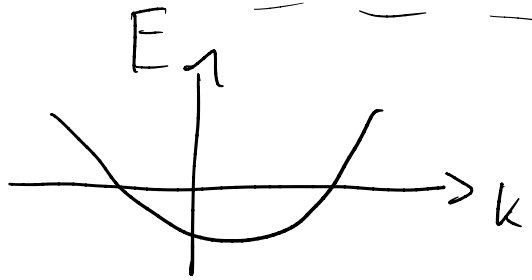


Nambu

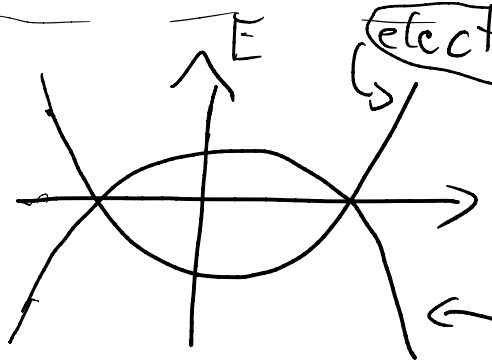


electron: $c^\dagger c$

hole $c c^\dagger$

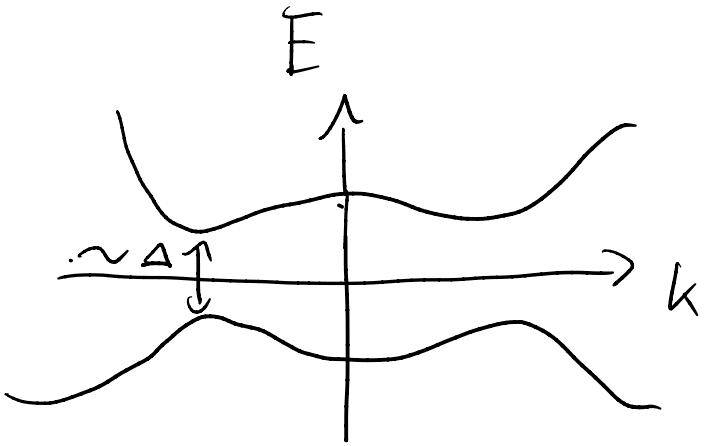


SC pairing

$\sim \Delta\, c_j c_{j+1} + h.c.$

$c_j^\dagger c_{j+1}^\dagger + h.c. = \frac{1}{2}(i \eta_j^\dagger \tilde{c}_y \eta_{j+1} + h.c.)$, and then

$$H'_{JW} = -h \sum_{j=1}^{L} \eta_j^\dagger \tilde{c}_z \eta_j - \frac{J}{2} \sum_{j=1}^{L-1} [\eta_j^\dagger (\tilde{c}_z + i\tilde{c}_y) \eta_{j+1} + h.c.]$$

$2L \times 2L$

or $H'_{JW} = \Psi^\dagger \mathbb{H} \Psi = (\eta_1^\dagger, \dots, \eta_L^\dagger)\, \mathbb{H} \begin{pmatrix} \eta_1 \\ \vdots \\ \eta_L \end{pmatrix}$

$$H = \begin{pmatrix} -h\hat{\tau}_z & -\frac{J}{2}(\hat{\tau}_x + i\hat{\tau}_y) & & & \\ -\frac{J}{2}(\hat{\tau}_x - i\hat{\tau}_y) & -h\hat{\tau}_z & & & \\ & & -h\hat{\tau}_z & & \\ & & & \ddots & \\ & & & & -h\hat{\tau}_z \end{pmatrix}$$

Associated Bloch-Hamiltonian:

$$h(k) = -J \sin k\, \hat{\tau}_y + (-h - J\cos k)\, \hat{\tau}_z$$

- Occurrence of edge states analogous to SSH model (see sheet 1, same equations have same solutions)
- GS-Energy: Sum over all single-particle energies $\varepsilon_n$ that have negative

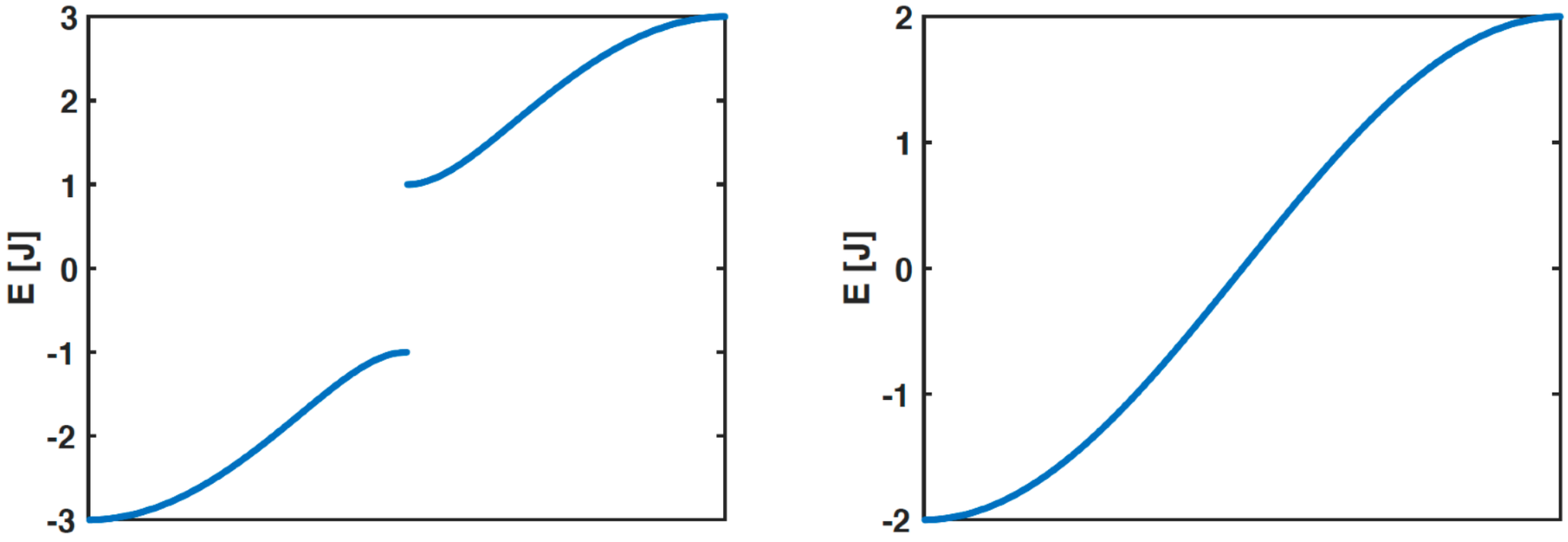


*Figure 1: Single-particle spectrum of (2.2) for $J = 1$ and $L = 300$. In the left panel $h = 2$, and the system is in a paramagnetic phase (for stronh $h$ the spins are polarized along the transverse magnetic field). In the right panel $h = 1$ and the single-particle energy gap closes. In the spin language this corresponds to the phase transition between paramagnetic phase ($h > J$) and the ferromagnetic phase when $h < J$.*

$$H'_{\rm JW} = -h \sum_{j=1}^{L} \eta_j^\dagger \, \tau_z \, \eta_j - \frac{J}{2} \sum_{j=1}^{L-1} \Big[ \eta_j^\dagger \left( \tau_z + i \tau_y \right) \eta_{j+1} + \text{h.c.} \Big] \, . \tag{2.2}$$

$$c_j^\dagger c_j = \frac{1}{2} \eta_j^\dagger \, \tau_z \, \eta_j + \frac{1}{2}$$

$$c_j^\dagger c_{j+1} + \text{h.c.} = \frac{1}{2} \Big( \eta_j^\dagger \, \tau_z \, \eta_{j+1} + \text{h.c.} \Big) \qquad \eta_j = \begin{pmatrix} c_j \\ c_j^\dagger \end{pmatrix} \, .$$

$$c_j^\dagger c_{j+1}^\dagger + \text{h.c.} = \frac{1}{2} \Big( i \, \eta_j^\dagger \, \tau_y \, \eta_{j+1} + \text{h.c.} \Big)$$

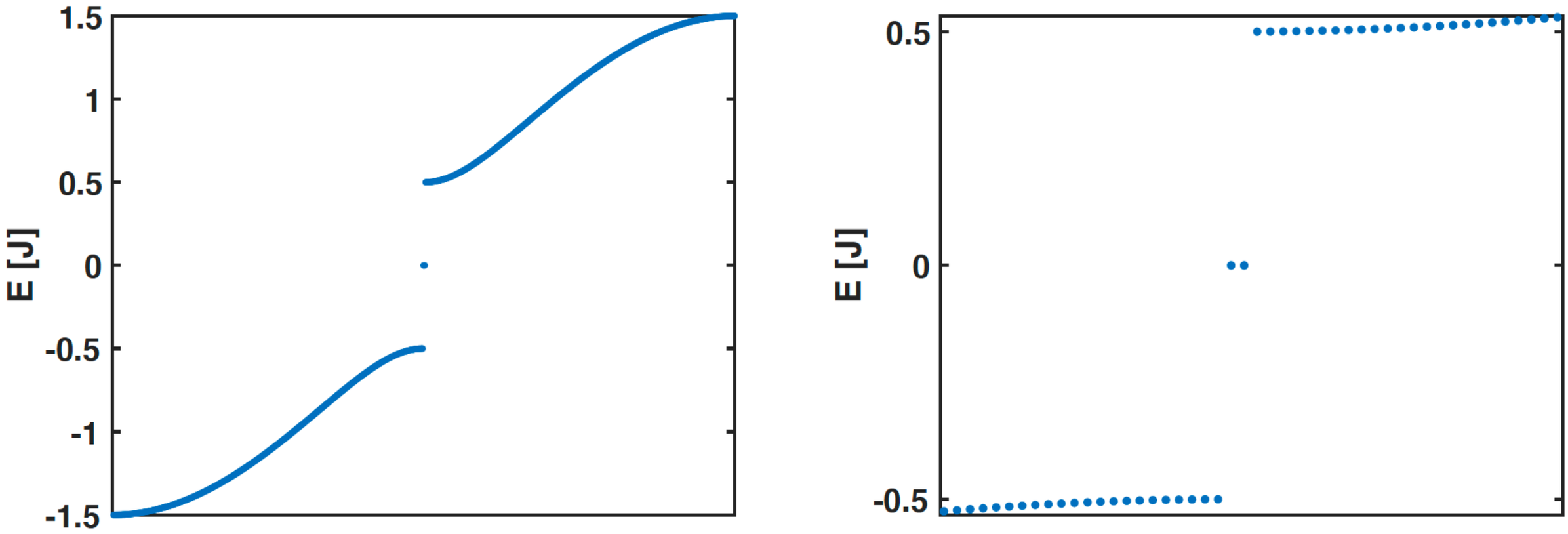


*Figure 2: Single-particle spectrum of (2.2) for $J = 1$ and $L = 300$, with $h = 0.5$, when the system is in the ferromagnetic phase (when $h = 0$ the system becomes a classical Ising chain). The right panel is a zoom of the two zero-energy modes appearing in the gap when $h < J$. The origin of these two zero-energy modes is difficult to understand in the spin language. In the fermionic language they are called Majorana modes, see [1] if you want to read more on the topic.*

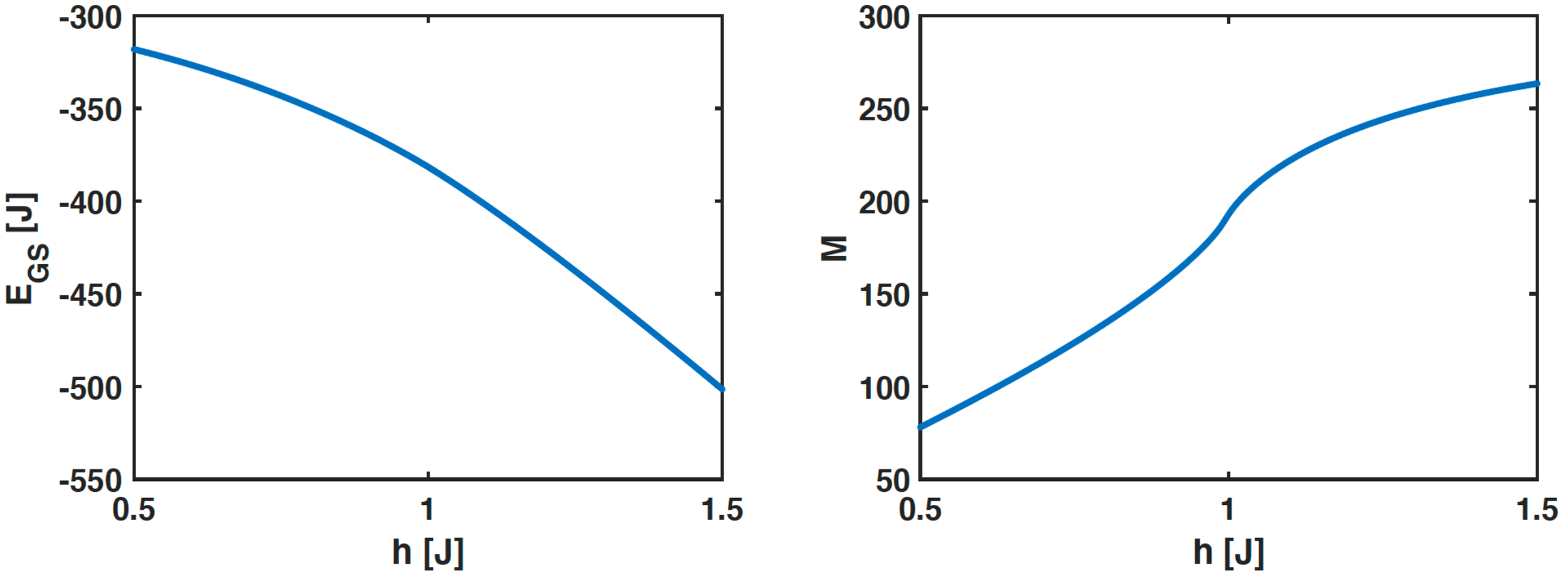


*Figure 3: Left panel: Ground-state energy as a function of* $h \in [0.5, 1.5]$ *with* $J = 1$. *Right panel: Ground-state transverse magnetization* $M$ *as a function of* $h \in [0.5, 1.5]$ *with* $J = 1$. *The length of the chain is fixed to* $L = 300$.

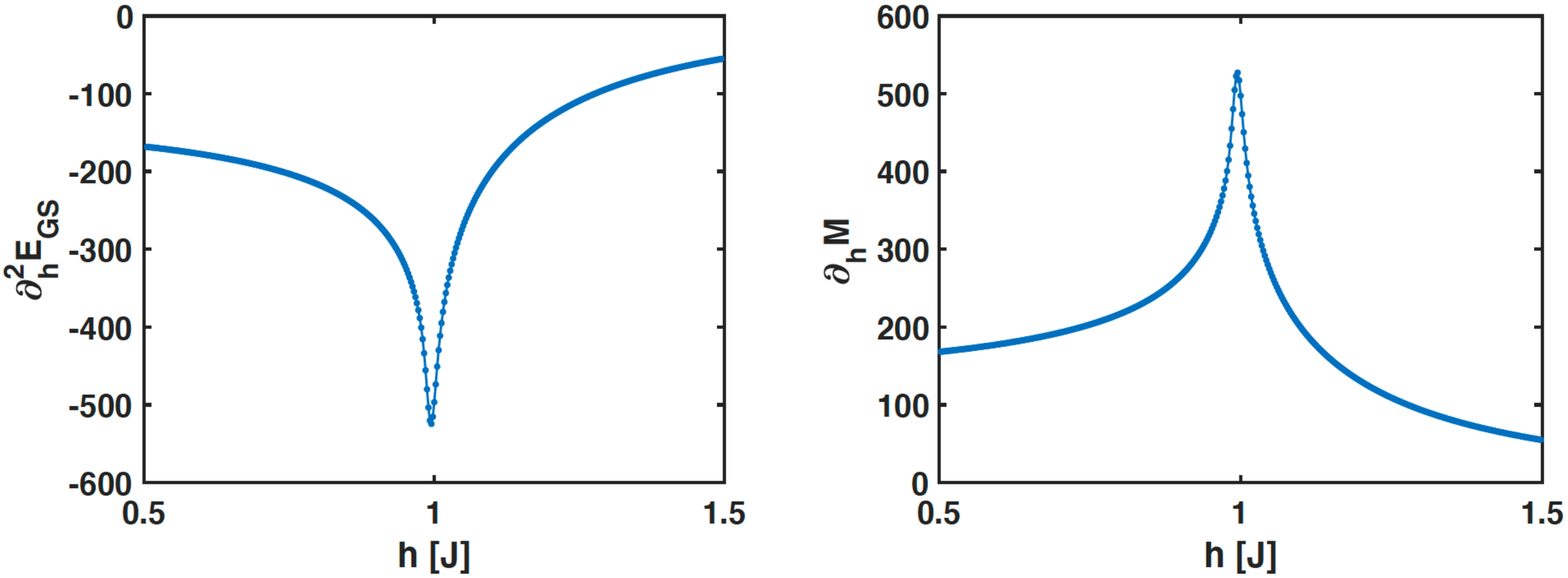


*Figure 4: Left panel: Second derivative of the ground-state energy w.r.t. $h$, in the interval $h \in [0.5, 1.5]$ with $J = 1$. Right panel: derivative of the ground-state transverse magnetization $M$ w.r.t. $h$, in the interval $h \in [0.5, 1.5]$ with $J = 1$. The length of the chain is fixed to $L = 300$. Notice the divercence occurring at the transition point between the ferromagnetic ($h < J$) and the paramagnetic ($h > J$) phases.*

eigenvalues.

- Magnetization $M = \sum_j \langle \sigma_j^z \rangle \overset{\partial W}{=} 2 \sum_j \langle c_j^\dagger c_j \rangle - L =$ (Nambu)

$$= \sum_j \langle \eta_j^\dagger \hat{\tau}_z \eta_j \rangle ,$$

where $\langle \eta_j^\dagger \tau_z \eta_j \rangle = \sum_{n \text{ occupied } (\varepsilon_n < 0)} \langle \phi_n | \left( |2j-1\rangle\langle 2j-1| - |2j\rangle\langle 2j| \right) |\phi_n\rangle$ (2L eigenv. of $\mathbb{H}$)

$$= \sum_{n \text{ occ}} \left( |\phi_n(2j-1)|^2 - |\phi_n(2j)|^2 \right)$$

- With $E_{GS} = \sum_{n \text{ occ}} \varepsilon_n$, calculate

$$\frac{\partial^2 E_{GS}(h)}{\partial h^2} = \frac{E_{GS}(h+\varepsilon) - 2E_{GS}(h) + E_{GS}(h-\varepsilon)}{\varepsilon^2}, \quad \varepsilon \sim 10^{-7}$$

$$\frac{\partial M(h)}{\partial h} = \lim_{\varepsilon \to 0} \frac{M\left(h+\frac{\varepsilon}{2}\right) - M\left(h-\frac{\varepsilon}{2}\right)}{\varepsilon}, \text{ put } \varepsilon \sim 10^{-7}.$$

3) ED with Lanczos on $H = -J \sum_i \sigma_i^z \sigma_{i+1}^z - h \sum_i \sigma_i^x$

- Binary representation of $H$:

  ↳ $-h \sum_i \sigma_i^x$ (see Lecture 7)

  ↳ $-J \sum_i \sigma_i^z \sigma_{i+1}^z$

---

jbit = $2^{L-i}$

jp1bit = $2^{L-i-1}$

Loop on $I$ : $0, \dots, 2^L - 1$ {

```
if ((jbit AND I) == (jp1bit AND I)) {
    H[I, I] += (-1);
} else { H[I, I] += (+1); }
}
```

- Implement Lanczos algorithm as discussed in Lecture 9.

  ⇝ Ground-state energies concur to cutoff-precision for all system sizes with free fermion solution.

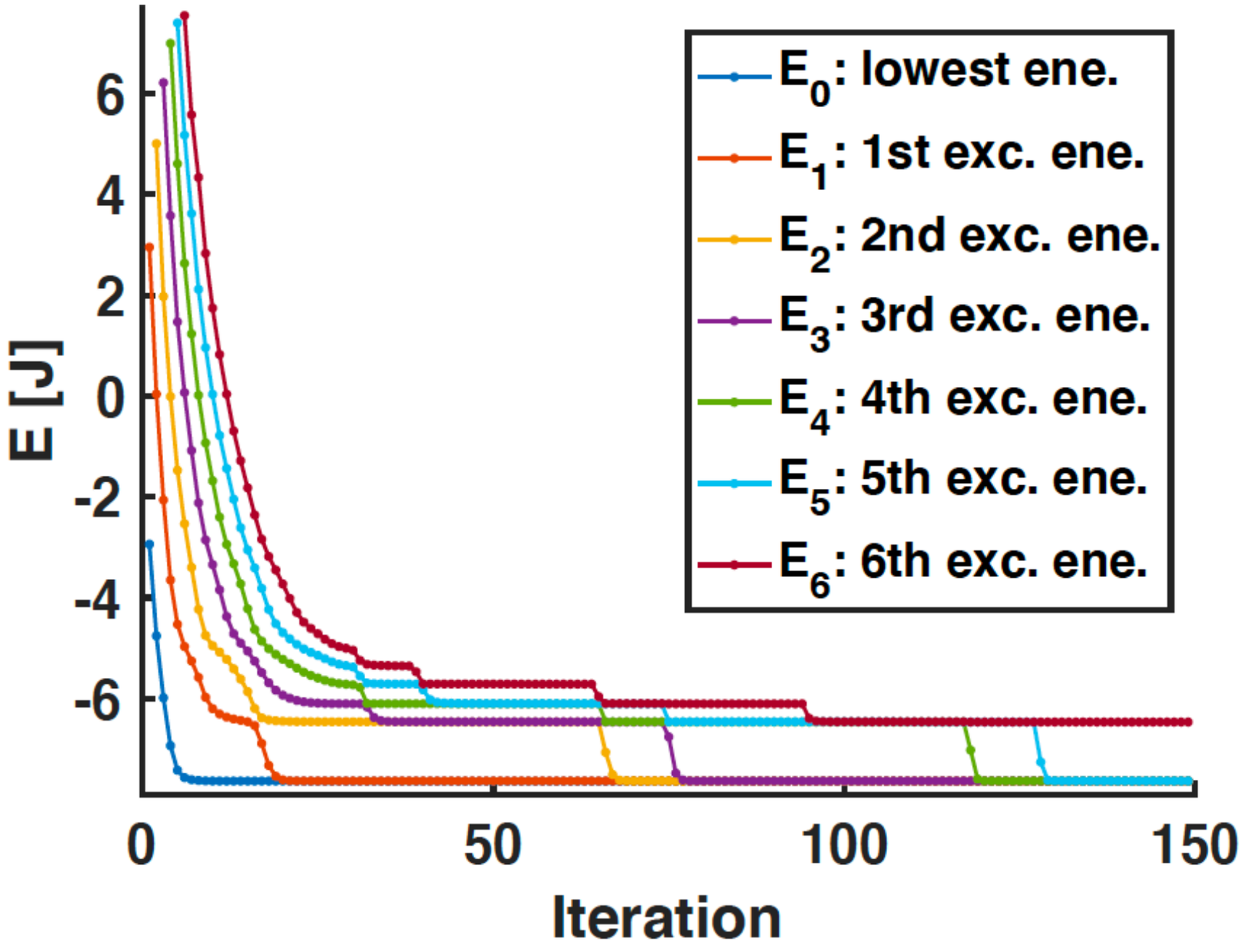


*Figure 5: Convergence plot of the 7 lowest eigenvalues using the Lanczos algorithm, for $L = 8$, $h = 0.5$ and OBC. Already after 50 iterations the ground-state energy is converged to numerical accuracy. For longer iteration times (after roughly 60) one can notice that higher lying eigenvalues start decaying to the ground-state energy, which signals the overconvergence of the Lanczos algorithm.*

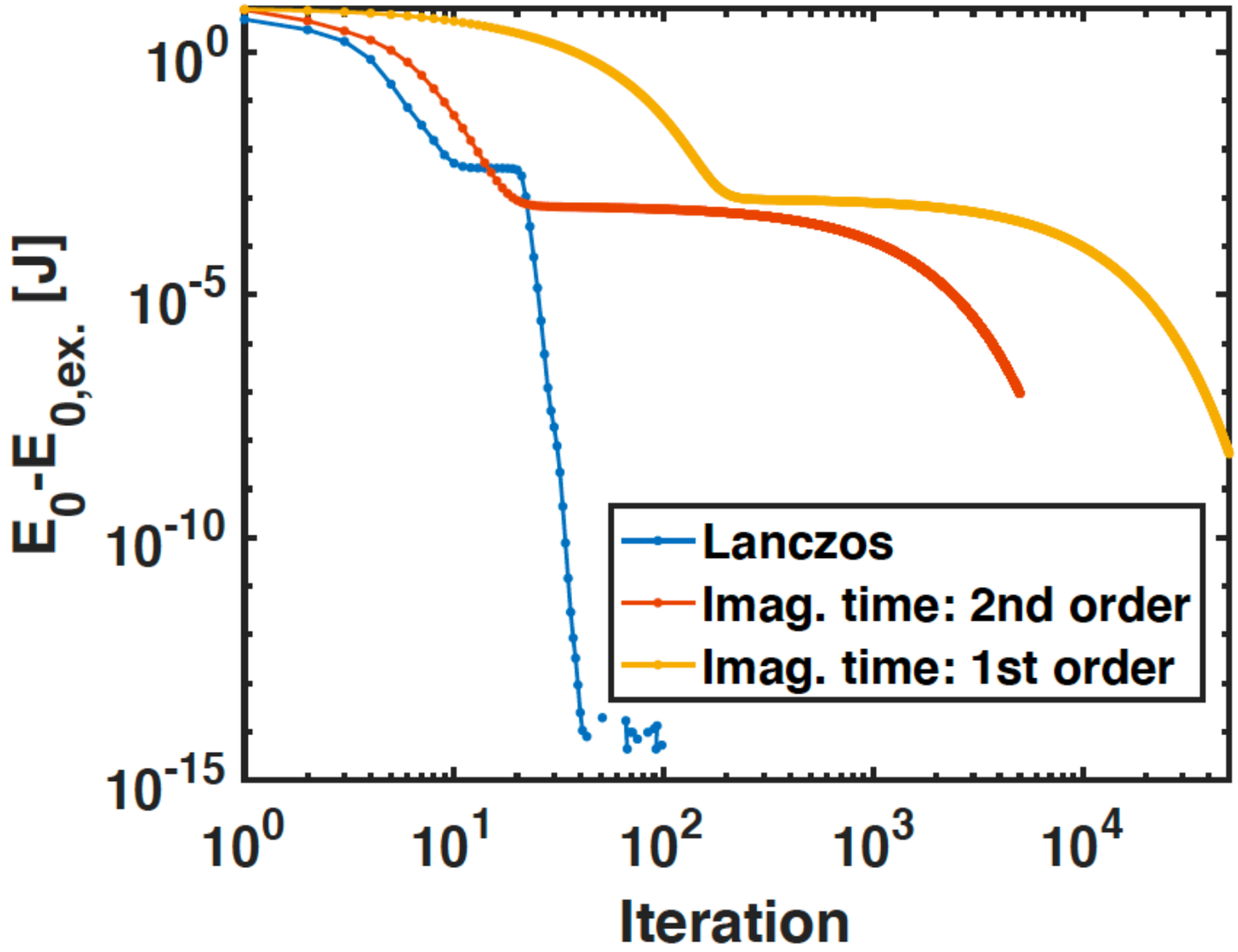


*Figure 6: Convergence plot of the Lanczos method (blue curve) compared with imaginary time evolution to $2^{nd}$ order accuracy (orange curve) and to $1^{st}$ order (yellow curve). On the $y$ axis the difference between the energy at the given iteration and the exact value of the ground-state energy obtained from the JW transformation is shown, for $L = 8$, $h = 0.5$ and OBC. For the Lanczos algorithm, already after 50 iterations the ground-state energy is converged to numerical accuracy. For the orange curve, the time step $\Delta\tau = 0.25$, whereas for the yellow curve $\Delta\tau = 0.025$, and for both, the total imaginary time duration is $1250\, J^{-1}$.*

4) Add $H_{int} = \lambda \sum_j \sigma_j^x \sigma_{j+1}^x$ to Hamiltonian, and do JW plus U-rotation:

$$H'_{JW} + H'_{int,JW} = hL - 2h \sum_{j=1}^{L} c_j^\dagger c_j - J \sum_{j=1}^{L-1} \left( c_j^\dagger c_{j+1} + c_j^\dagger c_{j+1}^\dagger + \text{h.c.} \right) + 4\lambda \sum_{j=1}^{L-1} \left( c_j^\dagger c_j - \frac{1}{2} \right)\left( c_{j+1}^\dagger c_{j+1} - \frac{1}{2} \right)$$

2-body interaction precludes exact "analytical" solution.

- Do Lanczos on $H + H_{int}$
  - Binary representation of $H_{int} = \lambda \sum_j \sigma_j^x \sigma_{j+1}^x$:

jjprbits = $2^{L-j} + 2^{L-j-1}$ ;

Loop on I : 0 --- $2^L - 1$ {

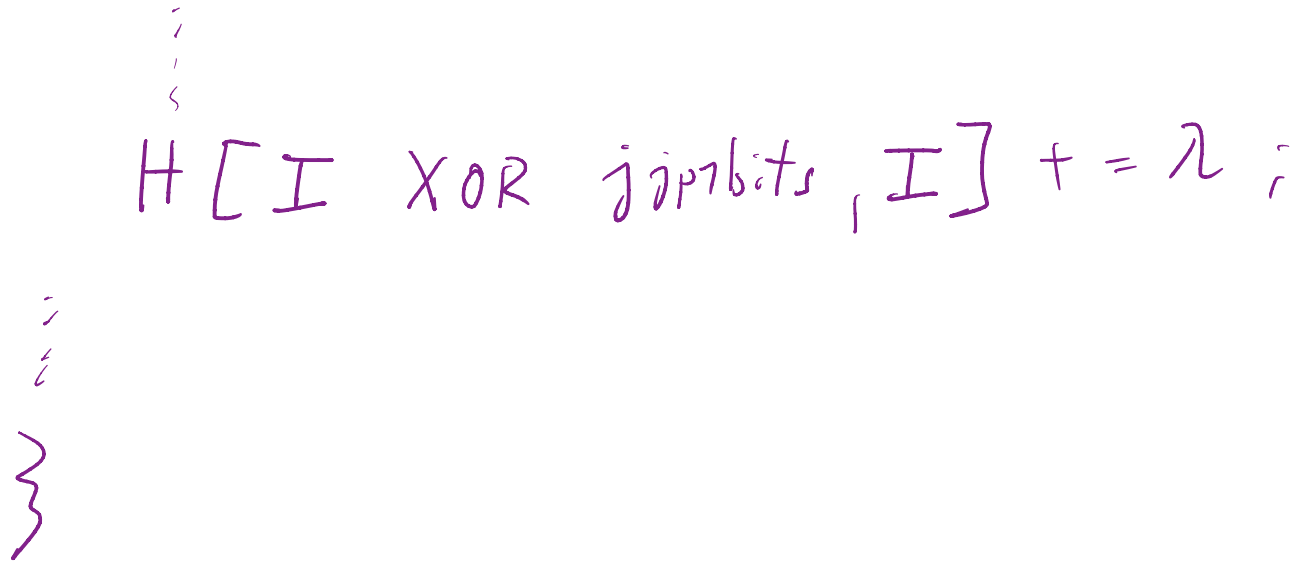


Compute h-2 phase diagram at J = 1.

Compare results to H. Katsura et al., PRB 92, 115 137 (2015), after identifying t = J; Δ = -J; μ = 2h, U = 2.

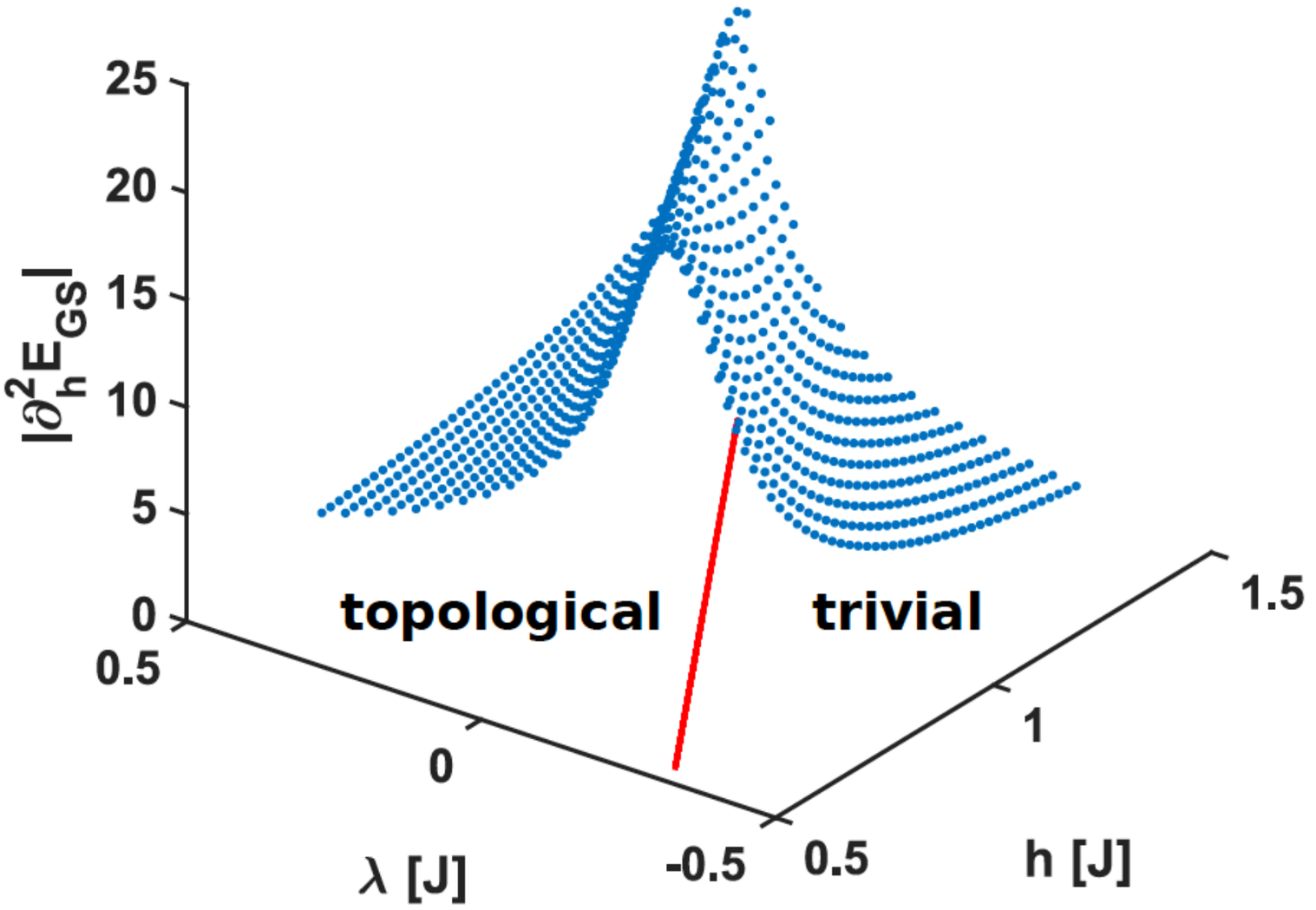


*Figure 7: Plot of* $\left|\frac{\partial^2 E_{GS}}{\partial h^2}\right|$ *as a function of* $h \in [0.5, 1.5]$ *and* $\lambda \in [-0.3, 0.3]$ *with* $J = 1$. *The length of the chain is fixed to* $L = 18$, *and PBC are used. Even for this length one can still see the diverging behavior of* $\frac{\partial^2 E_{GS}}{\partial h^2}$ *occurring at the phase transition. The red line marks the location of the maxima of* $\left|\frac{\partial^2 E_{GS}}{\partial h^2}\right|$, *and corresponds to the phase transition between the ferromagnetic (topological, in the fermionic language [5]) and the paramagnetic (trivial) phase. This phase transition line is approximate as one should perform a finite-size scaling of the location of the maxima to get more accurate results, but one can still qualitatively see that the interaction term (4.1) shifts the location of the phase transition. This qualitatively reproduces (a small portion of) the phase diagram shown in [5].*

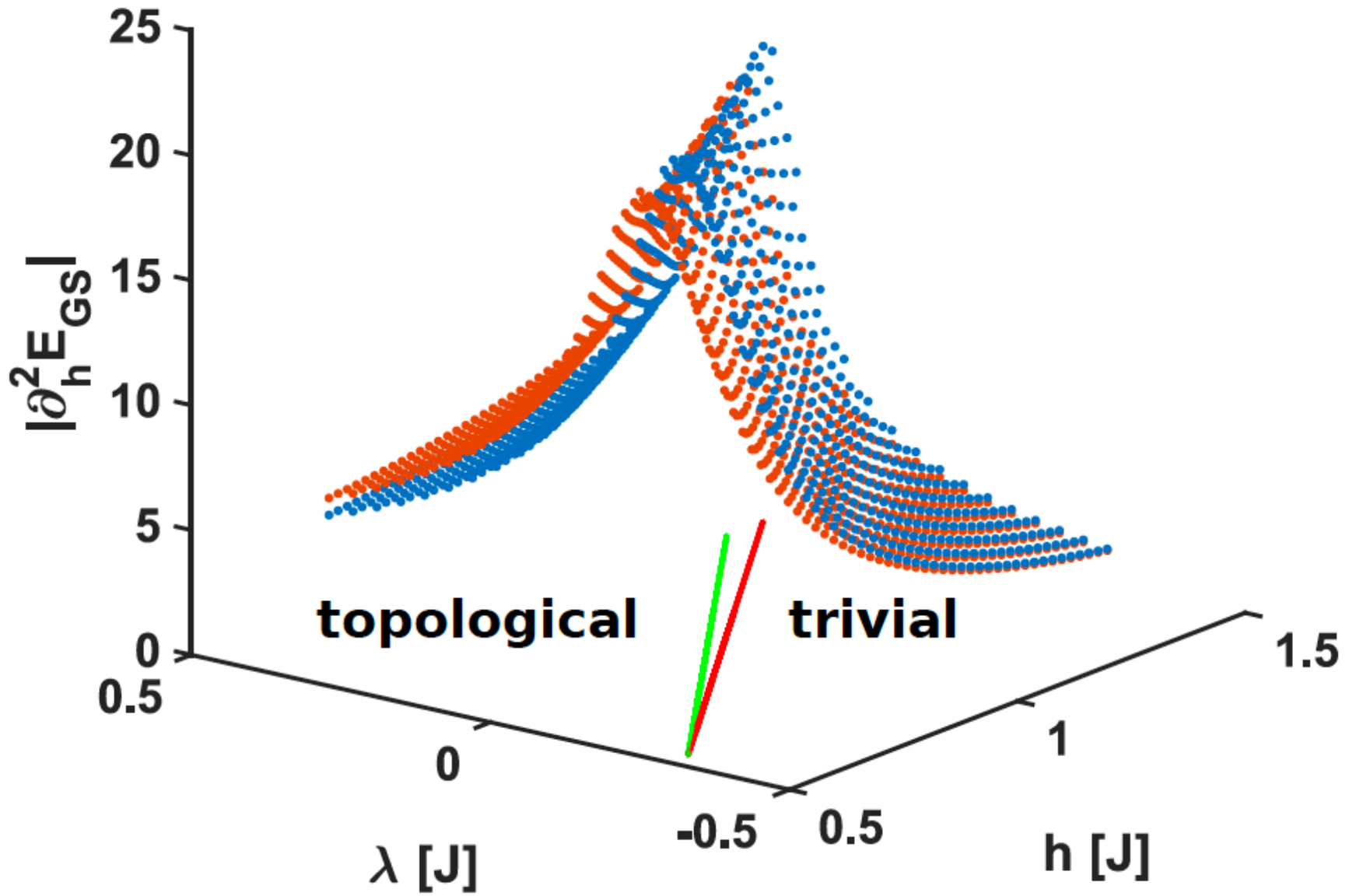


*Figure 8: Plot of* $\left|\frac{\partial^2 E_{GS}}{\partial h^2}\right|$ *as a function of* $h \in [0.5, 1.5]$ *and* $\lambda \in [-0.3, 0.3]$ *with* $J = 1$. *The length of the chain is fixed to* $L = 18$, *and a comparison between PBC (blue dots, and red line marking the maxima) and OBC (orange dots, and green line marking the maxima) is shown. The results for PBC are more accurate as finite size effects are less prominent. One could see that by plotting* $\left|\frac{\partial^2 E_{GS}}{\partial h^2}\right|$ *along the line* $\lambda = 0$*: for PBC the maximum is closer to* $h = 1$.

# References


[1] J. Alicea, *New directions in the pursuit of Majorana fermions in solid state systems*, Rep. Prog. Phys. **75**, 076501 (2012).

[2] H.Q. Lin, J.E. Gubernatis, *Exact Diagonalization Methods for Quantum Systems*, Computers in Physics **7**, 400 (1993).

[3] A. Weie, H. Fehske, *Exact Diagonalization Techniques*, in Lecture Notes in Physics **739**, *Computational Many-Particle Physics*, Springer (2007).

[4] E. Koch, *The Lanczos Method*, in *The LDA+DMFT approach to strongly correlated materials*, Forschungszentrum Jülich, Zentralbibliothek, Verlag (2011).

[5] H. Katsura, D. Schuricht, M. Takahashi, *Exact ground states and topological order in interacting Kitaev/Majorana chains*, Phys. Rev. B **92**, 115137 (2015).